NIH Public Access
Author Manuscript
Cell. Author manuscript; available in PMC 2015 January 30.

Published in final edited form as:
Cell. 2014 January 30; 156(3): 440–455. doi:10.1016/j.cell.2013.12.039.

Lung stem cell differentiation in mice directed by endothelial cells via a BMP4-NFATc1-Thrombospondin-1 axis

Joo-Hyeon Lee[1,2], **Dong Ha Bhang**[3], **Alexander Beede**[1,2], **Tian Lian Huang**[4], **Barry R. Stripp**[5], **Kenneth D. Bloch**[6], **Amy J. Wagers**[7], **Yu-Hua Tseng**[4], **Sandra Ryeom**[3], and **Carla F. Kim**[1,2,8]

[1] Stem Cell Program, Boston Children's Hospital, Boston MA 02115 and the Harvard Stem Cell Institute, Cambridge, MA 02138 USA

[2] Department of Genetics, Harvard Medical School, Boston, MA 02115 USA

[3] Department of Cancer Biology, Abramson Family Cancer Research Institute, U. Pennsylvania School of Medicine, Philadelphia, PA 19104.

[4] Section on Integrative Physiology and Metabolism, Joslin Diabetes Center, Harvard Medical School, Boston, MA,02215, USA; Harvard Stem Cell Institute, Harvard University, Cambridge, MA 02138, USA

[5] Women's Guild Lung Institute, Department of Medicine, Cedars-Sinai Medical Center, Los Angeles, CA 90048 USA

[6] Anesthesia Center for Critical Care Research and Cardiovascular Research Center, Massachusetts General Hospital, Boston, MA, 02114 USA

[7] Harvard Stem Cell Institute and Department of Stem Cell and Regenerative Biology, Harvard University, Cambridge, Massachusetts 02138, USA; Joslin Diabetes Center, Boston, MA 02215, USA; Howard Hughes Medical Institute

SUMMARY

Lung stem cells are instructed to produce lineage-specific progeny through unknown factors in their microenvironment. We used clonal three-dimensional (3D) co-cultures of endothelial cells and distal lung stem cells, bronchioalveolar stem cells (BASCs), to probe the instructive mechanisms. Single BASCs had bronchiolar and alveolar differentiation potential in lung endothelial cell co-cultures. Gain and loss of function experiments showed BMP4-Bmpr1a signaling triggers calcineurin/NFATc1-dependent expression of Thrombospondin-1 (*Tsp1*) in lung endothelial cells to drive alveolar lineage-specific BASC differentiation. *Tsp1*-null mice exhibited defective alveolar injury repair, confirming a crucial role for the BMP4-NFATc1-TSP1 axis in lung epithelial differentiation and regeneration in vivo. Discovery of this pathway points to methods to direct the derivation of specific lung epithelial lineages from multipotent cells. These findings elucidate a pathway that may be a critical target in lung diseases and provide new tools to understand the mechanisms of respiratory diseases at the single cell level.

© 2014 Elsevier Inc. All rights reserved.

[8] Corresponding author Contact information: carla.kim@childrens.harvard.edu Phone: 617-919-4644 Fax: 617-730-0222.

Publisher's Disclaimer: This is a PDF file of an unedited manuscript that has been accepted for publication. As a service to our customers we are providing this early version of the manuscript. The manuscript will undergo copyediting, typesetting, and review of the resulting proof before it is published in its final citable form. Please note that during the production process errors may be discovered which could affect the content, and all legal disclaimers that apply to the journal pertain.

Extended Experimental Procedures are available in Supplemental Information.

NIH-PA Author Manuscript
NIH-PA Author Manuscript
NIH-PA Author Manuscript

NIH-PA Author Manuscript

NIH-PA Author Manuscript

NIH-PA Author Manuscript

Keywords

Lung stem cells; Lineage; Differentiation; Endothelial cells; Tsp1; Bmp4

INTRODUCTION

Adult tissue stem cells reside in specialized niches containing supporting cells and factors that control stem cell survival, self-renewal and differentiation (Jones and Wagers, 2008; Morrison and Spradling, 2008). Lung epithelial repair is governed by stem/progenitor cell populations in distinct niches along the proximal-distal axis (e.g., Rawlins et al., 2009; Rock et al., 2011; Otto, 2002). Crosstalk between lung stem/progenitor cells and their niche is likely pivotal for maintaining the balance of stem and differentiated cells. Defects in such interactions may lead to acute respiratory distress syndrome, bronchopulmonary dysplasia, chronic obstructive pulmonary disease, idiopathic pulmonary fibrosis, and cancer. However, little is known about the supporting cells affecting lung regenerative potential or the precise mechanisms regulating differentiation and repair.

BronchioAlveolar Stem Cells (BASCs) are adult murine distal lung epithelial stem cells that reside in the bronchioalveolar duct junction, where the airways open to the alveolar space. BASCs co-express the bronchiolar club cell (Clara) marker, CCSP (club cell (Clara) secretory protein)(Scgb1a), and the Alveolar Type 2 cell (AT2) marker, SPC (pro-surfactant protein C) (Kim et al., 2005). Fluorescence activated cell sorting (FACS)-enriched BASCs self-renew and differentiate in two-dimensional culture systems and proliferate in response to bronchiolar and alveolar lung injury (Dovey et al., 2008; Kim et al., 2005; Zacharek et al., 2011). Lineage-tracing studies showed BASCs can give rise to alveolar epithelial cells in vivo (Rock et al., 2011; Tropea et al., 2012). Multiple stem/progenitor cell populations in the adult distal lung, including BASCs, club cells, AT2 cells, and integrin-alpha-6-expressing alveolar progenitors, may contribute to homeostasis and repair (Barkauskas et al., 2013; Chapman et al., 2011; Rawlins et al., 2009; Rock et al., 2011; Tropea et al., 2012). Clonal analysis of these cells has not been feasible, limiting understanding of lung stem cells.

3D Matrigel-based culture systems mimicking the niche have advanced the lung stem cell field. Distal lung epithelial stem/progenitor cells required support cells such as fibroblasts to form epithelial colonies (Kim et al., 2005; Lee et al., 2013; McQualter et al., 2010; Teisanu et al., 2011). The distal lung is highly vascularized, and numerous studies show an important role for the vasculature in lung development (DeLisser et al., 2006; Jakkula et al., 2000). Endothelial-derived Mmp14 is crucial for AT2 cell proliferation during lung regeneration (Ding et al., 2011). While these studies have laid an important framework, it is not known how lineage-specific differentiation of lung stem cells is regulated by stroma. Here we identify a BMP4-NFATc1-TSP1 signaling axis in endothelial cells that is critical for alveolar specification of BASC differentiation.

RESULTS

Lung endothelial cells support BASC stem cell properties

Given the intimate spatial relationship between lung epithelium and endothelial cells, we asked whether endothelial cells support 3D epithelial growth. CD31-CD45-EpCAM+Sca1- cells (enriched for AT2 cells, AT2 hereafter) or CD31-CD45-EpCAM+Sca1+ cells (enriched for putative BASCs, BASCs hereafter) from β-actin-GFP mice were co-cultured with primary mouse lung endothelial cells (LuMECs)(Figure 1A, S1A, and S1B). After 14 days, epithelial colonies were observed in AT2 cell and BASC co-cultures (Figure 1B). Limiting dilution assays showed LuMECs supported BASC self-renewal (Figure S1C);

NIH-PA Author Manuscript

NIH-PA Author Manuscript

NIH-PA Author Manuscript

BASCs were passaged multiple times in the presence of LuMECs without decreased colony-forming efficiency whereas AT2 cell colony formation decreased with passage (Figure 1C and S1C).

Importantly, LuMECs supported BASC differentiation into multiple epithelial lineages. Three colony types arose in BASC/LuMEC co-cultures: bronchiolar-like structures (bronchiolar colonies hereafter) with cells positive for CCSP; alveolar-like structures (alveolar colonies hereafter) expressing SPC; and mixed morphology structures (bronchioalveolar colonies hereafter, see below) containing CCSP-positive and SPC-positive cells (Figure 1B, 1D, and 1E). In contrast, AT2 cells only formed alveolar structures expressing SPC (Figure 1B, 1D, and 1E). Quantitative RT-PCR (qPCR) analysis confirmed the expression of CCSP and SPC in BASC colonies, yet no detectable expression of CCSP in AT2 cell colonies (Figure S1D). The alveolar type 1 (AT1) cell marker, T1α, and the ciliated cell marker, FoxJ1, were detected in BASC cultures while AT2 cultures only expressed SPC and T1α (Figure S1E). Bronchiolar colonies also contained ciliated cells positive for Acetylated-tubulin and goblet cells expressing MUC5AC (Figure S1F) but there was no expression of these markers in alveolar colonies (Figure S1G and data not shown). Mixed colonies contained cells positive for CCSP, Acetylated-tubulin, MUC5AC, or SPC, and CCSP- and SPC-dual positive cells (Figure S1H). We have termed mixed colonies, “bronchioalveolar colonies.” LuMECs also supported BASC differentiation after subcutaneous co-transplantation. BASCs, but not AT2 cells, co-injected with LuMECs formed tube-like structures lined by epithelial cells expressing CCSP, SPC, or both (Figure 1F). These data suggested that LuMECs support BASC self-renewal and differentiation into bronchiolar and alveolar lineages in vitro and in vivo.

The derivation of multiple lineages in 3D co-cultures could be a result of multipotent stem cell differentiation or the outgrowth of a mixture of cell types. BASCs from GFP or DsRed mice were mixed and co-cultured with LuMECs. Colonies that arose were green or red, suggesting their clonal nature (Figure S1I). To further test multipotency, individual colonies were tested for secondary colony formation and differentiation (Figure 1G). Bronchioalveolar colonies gave rise to all 3 colony types with repeated passage, while bronchiolar colonies generated only bronchiolar colonies and alveolar colonies only formed alveolar colonies (Figure 1H, 1I, 1J, S1K, and S1L). Bronchioalveolar colonies retained efficient colony formation compared to bronchiolar colonies, and alveolar colonies had limited passaging capacity (Figure S1J and S1M). Bronchioalveolar colonies from BASC/LuMEC cultures also exhibited multipotent differentiation capacity in vivo, since they produced numerous lung epithelial structures consisting of Acetylated-tubulin-, MUC5AC-, CCSP-, SPC-, or dual-positive CCSP/SPC cells after subcutaneous transplantation (Figure 1I, S1N, and S1O). Bronchiolar colonies generated rare epithelial structures while alveolar colonies were unable to form epithelial structures (Figure 1I).

The ability of single cells to give rise to multiple lineages is a stem cell hallmark that has not been demonstrated in lung 3D co-cultures. Single BASCs from GFP mice were co-cultured with LuMECs and DsRed-labeled “helper cells” (irradiated EpCAM+ lung epithelial cells) (Figure 2A). Single BASCs developed colonies of all 3 types, with bronchioalveolar colonies the predominant type (80%)(Figure 2B and 2C). IF confirmed the multi-lineage differentiation of these bronchioalveolar colonies (Figure 2D) with the continued ability to differentiate after multiple passages (Figure 2E and 2F).

Endothelial cells govern BASC differentiation in an organ-specific manner

Organ-specific endothelium has been implicated in other stem cell niches so we isolated primary liver endothelial cells (LiMECs) (Figure S2) and co-cultured them with BASCs. BASC/LiMEC co-cultures had enhanced bronchiolar colony formation and reduced alveolar

NIH-PA Author Manuscript

NIH-PA Author Manuscript

NIH-PA Author Manuscript

colony formation compared to BASC/LuMEC co-cultures (Figure 3A, 3B, and 3C). Passaged bronchioalveolar colonies also exhibited markedly expanded bronchiolar colony differentiation at the expense of alveolar colonies when co-cultured with LiMECs (Figure 3D). Bronchioalveolar colonies arising from BASC/LuMEC co-cultures were subcutaneously injected with LuMEC or LiMEC. LiMEC co-injections yielded primarily bronchiolar structures in contrast to the 3 different types of lung epithelial structures formed in LuMEC co-injections (Figure 3E and 3F), suggesting a specific requirement for lung endothelium in BASC differentiation.

TSP1 in endothelial cells regulates BASC differentiation

The necessity of lung endothelial cells in BASC differentiation suggested that endothelial factors are important for this process. TSP1, an angiogenesis inhibitor, is highly expressed in lung endothelial cells (Adams and Lawler, 2004; Chen et al., 2000; Lawler, 2002) and is up-regulated developmentally when alveolar epithelial cells proliferate and differentiate (Iruela-Arispe et al., 1993; O'Shea and Dixit, 1988). Since TSP1 expression was significantly higher in LuMECs versus LiMECs (Figure 3G), we examined its role in BASC differentiation.

Lung injury models can identify proteins necessary for lung regeneration and differentiation. LuMECs were isolated at various times after naphthalene or bleomycin treatment, in vivo models of bronchiolar and alveolar epithelial injury, respectively, to examine *Tsp1* expression. *Tsp1* mRNA was significantly reduced in LuMECs 3 days after naphthalene treatment when regeneration of club cells occurs and restored 14 days after injury when regeneration is largely completed (Figure 4A). In contrast, bleomycin treatment led to higher *Tsp1* expression in LuMECs 14 days after injury when alveolar epithelial repair is underway (Figure 4A).

To gain insight into the necessity of TSP1 as a regulator of BASC differentiation, we tested *Tsp1*-deficient LuMECs in 3D co-cultures. LuMECs were isolated from $Tsp1^{-/-}$ mice (Lawler et al., 1998). $Tsp1^{-/-}$ LuMECs modestly increased colony number in co-cultures (Figure S3A). Strikingly, BASC/$Tsp1^{-/-}$ LuMEC co-cultures produced 3.2-fold more bronchiolar colonies and 3.5-fold fewer alveolar colonies than BASC/$Tsp1^{+/+}$ LuMEC co-cultures (Figure 4B and 4C). CCSP and SPC mRNA levels validated the enhanced bronchiolar differentiation phenotype with $Tsp1^{-/-}$ LuMECs (Figure 4D). Altered differentiation was not due to a lineage-specific proliferation defect, as bronchiolar or alveolar colonies co-cultured with $Tsp1^{-/-}$ LuMECs actually showed increased colony numbers (Figure S3B) and generated bronchiolar or alveolar colonies, respectively, as expected (Figure 4E). $Tsp1^{-/-}$ BASCs exhibited differentiation capacity comparable to $Tsp1^{+/+}$ BASCs (Figure S3I). Normal bronchiolar and alveolar differentiation was seen when equal numbers of $Tsp1^{+/+}$ and $Tsp1^{-/-}$ LuMECs were mixed for co-culture with BASCs (Figure S3C, S3D, and S3E). Finally, subcutaneous co-transplantation of bronchioalveolar colonies with $Tsp1^{-/-}$ LuMECs yielded a significantly higher proportion of bronchiolar epithelial structures at the expense of alveolar structures compared with $Tsp1^{+/+}$ LuMEC co-injections (Figure 4F, 4G, and 4H). Together, these data strongly suggested TSP1 functions as a positive regulator of alveolar differentiation of BASCs in vitro and in vivo.

It was unclear if TSP1 played a direct role or if a downstream factor affected BASC differentiation. TSP1 constitutes a major portion (~20%) of total platelet α granule content during platelet activation (Baenziger et al., 1971; Ganguly, 1971; Lawler et al., 1978). The addition of $Tsp1^{+/+}$ platelet releasate ($Tsp1^{+/+}$ PR) to BASC/$Tsp1^{-/-}$ LuMEC co-cultures increased alveolar colony formation and reduced bronchiolar colonies compared to controls (Figure S3F, S3G, and S3H). Purified TSP1 protein from activated human platelets (native TSP1) added to BASC/$Tsp1^{-/-}$ LuMEC co-cultures similarly increased alveolar colony

NIH-PA Author Manuscript

NIH-PA Author Manuscript

NIH-PA Author Manuscript

formation as compared to treatment with vehicle alone (Figure S3G and S3H). These data demonstrate that with endothelial cells, TSP1 is sufficient to directly influence BASC alveolar differentiation.

BMP4 induces BASC alveolar differentiation in an organ-specific manner

TSP1 is a multifunctional glycoprotein with numerous receptors, however control of TSP1 expression is not well understood. We isolated LuMECs at various times after naphthalene or bleomycin injury and analyzed 15 growth factors known to function in lung development or stem cell cultures (Figure S4A-S4D and data not shown). Three factors, *Hgf*, *Tgfβ1*, and *Bmp4*, showed a similar expression pattern as *Tsp1*; they were down-regulated after naphthalene injury and up-regulated after bleomycin injury (Figure S4A-S4D, Figure 5A, compare to Figure 4A). To investigate their influence on BASC differentiation, we added recombinant proteins to BASC/LuMEC co-cultures. BMP4 treatment led to the formation of significantly more alveolar colonies and fewer bronchiolar colonies, while TGFβ1 inhibited BASC colony formation and HGF had no effect (Figure 5B and 5C, data not shown). TSP1 was required for BMP4-induced alveolar differentiation; when BMP4 was added to BASC co-cultures with *Tsp1*$^{-/-}$ LuMECs, there was no increase in alveolar colonies (Figure 5B and 5C). BMP4 treatment correlated with activation of Smad1/5 and Erk1/2 signaling and up-regulation of *Tsp1* mRNA and protein levels in LuMECs (Figure S4E, S4F, S4G, 5D, and 5E). *Tsp1* expression and alveolar differentiation were reduced after treatment with the BMP inhibitor, Noggin (NOG)(Figure 5D, 5E, and S4G). The addition of BMP4 to BASC/LiMEC co-cultures did not increase *Tsp1* expression, nor did it increase alveolar colony formation (Figure 5B, 5C, 5D, 5E, S4E, and S4G). Thus, BMP4 treatment specifically induced *Tsp1* in lung endothelial cells.

We recently identified *Tsp1* as a direct target of transcription factor NFATc1 (nuclear factor of activated T cell c1) downstream of calcineurin activation (Ryeom Lab, unpublished data). We asked whether TSP1 induction and BASC differentiation employed the calcineurin-NFAT signaling pathway. Calcineurin is a serine/threonine phosphatase activated by increases in intracellular Ca^{2+} thus we monitored calcium influx after BMP4 addition using the Ca^{2+} indicator Fluo-4 AM. Within 1min, BMP4 treatment significantly increased the intensity of Fluo-4 as did VEGF, a known activator of calcineurin signaling (Figure 5F and Movie S1) (Barkauskas et al., 2013; Hesser et al., 2004; Minami et al., 2004). To confirm BMP4 stimulated NFATc1 activation, NFATc1 localization was assessed by IF. NFATc1 localized to the nucleus in LuMECs within 10 minutes after BMP4 treatment and was re-exported to the cytoplasm after NOG treatment (Figure 5G and S4H). In contrast, NFATc1 expression and localization was unaltered by BMP4 or NOG in LiMECs (Figure 5G).

Overexpression of a constitutively active NFATc1 (CaNFATc1) or treatment with ionomycin to activate calcineurin in LuMECs strongly induced *Tsp1* expression, indicating that NFATc1 acts upstream of *Tsp1* (Figure 5E and S4H). Further, addition of the specific calcineurin inhibitor, cyclosporin A (CsA), to BASC/LuMEC co-cultures significantly abrogated the BMP4-dependent up-regulation of *Tsp1* expression and NFATc1 nuclear translocation (Figure 5D, 5E, 5G). In the presence of CsA and BMP4, BASC/LuMEC co-cultures yielded more bronchiolar colonies (Figure 5H). In contrast, BASCs co-cultured with CaNFATc1-LuMECs produced significantly more alveolar colonies compared to controls (Figure 5H). CsA did not affect Smad1/5 and Erk1/2 signaling (Figure S4G).

To define BMP4-induced direct interactions of NFATc1 with *Tsp1* in LuMECs, we assessed NFATc1 binding to the *Tsp1* promoter by Chromatin Immunoprecipitation (ChIP). In BMP4-treated LuMECs but not LiMECs, NFATc1 ChIP showed significant enrichment of *Tsp1* (Figure 5I). Binding of NFATc1 on the *Tsp1* promoter was disrupted in LuMECs

NIH-PA Author Manuscript

NIH-PA Author Manuscript

NIH-PA Author Manuscript

treated with BMP4 + NOG (Figure 5I). These data suggest that in response to BMP4, NFATc1 activation is sufficient for TSP1-induced BASC alveolar differentiation.

Bmpr1a is required for BMP4-mediated TSP1 induction in LuMECs

To identify the critical BMP receptor for BMP4-mediated BASC regulation, we tested expression of known BMP receptors in LuMECs and found that *Acvrl1*, *Bmpr1a*, and *Bmpr2*, were highly expressed whereas *Acvr1*, *Bmpr1b*, *Acvr2a*, or *Acvr2b* showed little or no expression (Figure S5A and S5B). *Bmpr1a* was upregulated in LuMECs, but not in LiMECs, after BMP4 treatment (Figure S5A). These data, and previous work linking *Bmpr1a* and NFATc1 to regulation of hair follicle stem cells (Horsley et al., 2008), prompted us to further examine *Bmpr1a* in BASC differentiation.

To test the role of *Bmpr1a* in BASC/LuMEC co-cultures, LuMECs were isolated from *Bmpr1a*$^{f/f}$ mice followed by infection with Adenovirus-empty vector (Ad-Emp) or Adenovirus-Cre recombinase (Ad-Cre). Loss of *Bmpr1a* expression was confirmed by qPCR (Figure 6A). BASCs co-cultured with *Bmpr1a*-depleted LuMECs showed impaired alveolar differentiation; BASC/*Bmpr1a*$^{f/f}$*;* Ad-Cre LuMEC produced 4.6-fold more bronchiolar colonies and 1.4-fold fewer alveolar colonies than controls (Figure 6B). *Bmpr1a*-deficiency led to 2.42-fold less *Tsp1* mRNA in Cre-treated *Bmpr1a*$^{f/f}$ LuMECs than controls and reduced Tsp1 induction up to 12 hours after BMP4 treatment (Figure 6C and 6D). Finally, BMP4-induced nuclear translocation of NFATc1 was impaired in *Bmpr1a*-depleted LuMECs (Figure 6E). These data supported a model whereby BMP4 activates calcineurin/NFATc1 signaling through *Bmpr1a* to induce TSP1 expression in LuMECs.

Given its role in BASC differentiation, we asked whether *Bmpr1a* also played a role in lung injury repair. *Bmpr1a* expression levels were assayed in LuMECs at various time points following naphthalene and bleomycin injury. While there was no remarkable change after naphthalene, a significant increase in *Bmpr1a* expression (4.8-fold $p<0.01$) was seen at 14 days following bleomycin treatment (Figure 6F). Changes in Bmp signaling were also observed during lung epithelial regeneration; phosphorylated Smad1/5 and Erk1/2 was detected in LuMECs from uninjured mice and during bleomycin injury repair, whereas these phosphorylated proteins were decreased during naphthalene injury repair and undetectable in LiMECs (Figure S5C and S5D).

We probed epithelial cells as a source of BMP4 after lung injury and found that in homeostatic conditions, *Bmp4* expression was higher in AT2 cells and BASCs compared to total lung cells (Figure 6G). 3 days after naphthalene treatment, *Bmp4* expression was down-regulated in AT2 cells and BASCs, returning to baseline 14 days after injury (Figure 6G). In contrast, BASCs expressed 2.7-fold higher levels of *Bmp4* 14 days after bleomycin compared to controls ($p<0.01$) and AT2 cells showed 1.5-fold increased *Bmp4* expression 21 days after bleomycin ($p<0.01$ vs PBS)(Figure 6G). These results suggest that alveolar injury triggers *Bmp4* induction in BASCs, AT2 cells, or other epithelial cells, subsequently upregulating *Tsp1* from lung endothelial cells to control BASC differentiation in a Bmpr1a-calcineurin-NFATc1 dependent manner.

Altered bronchiolar and alveolar injury repair in *Tsp1*-null mice

Our studies identify TSP1 as a key regulator of lung stem cell differentiation, thus we tested the effects of *Tsp1* deficiency on bronchiolar epithelial repair. We first confirmed that *Tsp1*$^{-/-}$ mice (Lawler et al., 1998) did not exhibit a lung phenotype without injury (Figure S6A). IF analysis confirmed sufficient club cell ablation in *Tsp1*$^{+/+}$ and *Tsp1*$^{-/-}$ mice 2 days after naphthalene treatment (Figure 7A and 7B). Club cell numbers remained low 5-7 days after naphthalene in *Tsp1*$^{+/+}$ mice, whereas *Tsp1*$^{-/-}$ mice exhibited significantly more club

NIH-PA Author Manuscript

NIH-PA Author Manuscript

NIH-PA Author Manuscript

cells at these time points (Figure 7A and 7B). Interestingly, the number of BASCs peaked earlier in *Tsp1*$^{-/-}$ mice in response to naphthalene (Figure 7C).

Intratracheal administration of bleomycin selectively ablates AT2 cells (Aso et al., 1976) thus we evaluated the requirement for TSP1 during alveolar injury repair. IF analysis revealed a 4.4-fold reduction in SPC-expressing AT2 cells after bleomycin treatment in *Tsp1*$^{-/-}$ mice (Figure 7D and 7E). Numerous BrdU-labeled AT2 cells were observed in wild-type mice, yet *Tsp1*$^{-/-}$ mice had fewer BrdU-positive cells (Figure 7D). A slight yet significant increase in fibrosis was seen in *Tsp1*$^{-/-}$ mice compared to wild-type mice (Figure 7F and S6B), consistent with previous reports (Ezzie et al., 2011). The number of BASCs in *Tsp1*$^{+/+}$ mice increased 14 days after injury and declined to base line after 28 days (Figure 7G and 7H as expected (Kim et al., 2005). However, *Tsp1*$^{-/-}$ mice showed increased numbers of BASCs through 28 days after injury (Figure 7G and 7H). These data demonstrate a defect in alveolar epithelial repair in *Tsp1* deficiency and suggested that BASCs failed to sufficiently differentiate in response to alveolar injury.

We examined the sufficiency of endothelial-derived TSP1 for BASC alveolar differentiation following bleomycin injury. Conditioned medium (CM) collected from wild-type LuMECs, wild-type LiMECs or *Tsp1*$^{-/-}$ LuMECs (Figure S6C) was administered following bleomycin treatment. *Tsp1*-null mice treated with wild-type LuMEC CM exhibited AT2 cell regeneration comparable to wild-type mice; a 3-fold increase in SPC+ cells was observed in CM- versus media-treated *Tsp1*-null mice (Figure S6D and S6E). Neither CM from *Tsp1*$^{-/-}$ LuMECs or CM from wild-type LiMECs facilitated AT2 cell regeneration in *Tsp1*$^{-/-}$ mice (Figure S6D and S6E). CM from wild-type LuMECs also reduced fibrosis in *Tsp1*-null mice (Figure S6F) and restored BASC numbers comparable to those in wild-type mice (Figure S6G and S6H). Taken together, LuMEC-derived TSP1 was sufficient for repair of alveolar epithelial injury via regulation of BASC differentiation.

DISCUSSION

We have defined a signaling pathway that specifies lung stem cell differentiation. Endothelial cells supported BASC differentiation into multiple epithelial lineages in vitro and after subcutaneous injection. Using these 3D platforms, we identified a BMP4-controlled NFATc1-TSP1 axis in lung endothelial cells that directs BASC differentiation to the alveolar lineage. This endothelial-epithelial crosstalk is one mechanism by which lung stem cell differentiation choices are regulated in response to lung injury in vivo.

The differentiation capacity we uncovered in endothelial cell-supported 3D co-cultures and co-transplantations strengthens the stem cell identity of BASCs. Single FACS-purified BASCs were capable of multi-lineage differentiation. The degree to which these cells represent dual positive CCSP+ SPC+ cells in vivo remains an outstanding question. Further interrogation using in vivo systems to specifically label BASCs in their microenvironment remains an important goal. This work and previous studies provide evidence that distinguishes BASCs from other lung stem/progenitors, making it unlikely other cell populations contributed to our findings: basal cells from the upper airways do not require stromal cells for growth in 3D cultures (Rock et al., 2009), Sca1-low bronchiolar stem cells do not produce cells with alveolar phenotypes (Teisanu et al., 2011), and the SPC-negative Integrin-α6β4-positive progenitors may be restricted to alveolar lineages (Chapman et al., 2011). Direct comparisons of BASCs with other lung stem/progenitor populations could reveal that the BMP4-NFATc1-TSP1 signaling axis is broadly important for differentiation control in the distal lung.

NIH-PA Author Manuscript

NIH-PA Author Manuscript

NIH-PA Author Manuscript

Our results suggest that a BMP4-NFATc1-TSP1 signaling axis operates between stem cells, epithelial cells and endothelial cells to repair of lineage-specific injury in an organ-specific context. Our data and previous reports lead us to hypothesize that the lung epithelial injury repair signaling cascade begins with sensing changes in BMP4 and/or other additional molecules expressed by BASCs and distal lung epithelial cells (Masterson et al., 2011; Rosendahl et al., 2002; Sountoulidis et al., 2012). BMP4 appears to primarily act in lung endothelial cells by stimulating calcineurin and altering NFATc1 localization. Phosphorylation of SMAD1/5 and ERK1/2 and increased *Nfatc1* transcript were also detected after Bmp4 treatment in vitro and in vivo, suggesting canonical Bmp transcriptional responses also play a role in this setting. *Tsp1* expression is upregulated then secreted by lung endothelial cells signaling back to BASCs. It remains to be determined which TSP1 receptors and downstream signaling molecules regulate alveolar differentiation. The role of Tsp1 in lung injury repair may also involve interactions between other cell types aside from endothelial cells, and other endothelial factors or a structural role from endothelia may also be critical. Finally, in the absence of a known human BASC equivalent, it is unknown if a BMP4-NFATc1-TSP1 pathway operates in human lungs.

This work reveals that manipulation of the microenvironment can direct the lineage-specific differentiation of lung stem cells, an important proof of principle for therapeutic development for lung diseases. Whereas seminal strides have been made to differentiate iPS cells to lung cells (Green et al., 2011; Longmire et al., 2012; Mou et al., 2012), directed differentiation to produce a specific lung epithelial lineage is not yet possible. Our work identifies molecules, such as TSP1, that could be used to specify alveolar epithelial differentiation from adult multipotent stem cells. We and others have begun to identify key differences between organ-specific endothelia that may reveal additional molecules for differentiation control (Nolan et al., 2013). Injured or depleted lung epithelial cells are the hallmark of numerous pulmonary diseases, including alveolar damage in pulmonary fibrosis and bronchiolar ablation in bronchiolitis obliterans. Drugs that promote the relevant lineage-specific differentiation activity of lung stem cells might be useful in stimulating repair of patients' damaged lung cells. For example, drugs driving alveolar differentiation might aid fibrosis patients whereas chemicals promoting bronchiolar differentiation may help those with bronchiolitis obliterans patients. The organ-specific BMP4-NFATc1-TSP1 axis in lung endothelial cells we defined could be a new therapeutic avenue for these and other numerous lung diseases. Further elucidation of the networks that regulate BASCs could identify new potential drug targets for lung disease in stem cells and their interacting niche including endothelial cells.

EXPERIMENTAL PROCEDURES

Endothelial cell preparation

Lung endothelial cells (LuMECs) and liver endothelial cells (LiMECs) were isolated from 2-4 week old mice by negative selection with anti-CD45-conjugated magnetic beads and positive selection with anti-CD31-conjugated magnetic beads. CD31-positive cells were then amplified in a gelatin-coated culture plate for 3-5 days followed by reselection with anti-CD31-conjugated magnetic beads. Endothelial cell purity was determined by IF staining for CD31, VE-Cadherin and VEGFR2, and cells were used for experiments between passages 2 and 6. For Ac-LDL uptake, endothelial cells were incubated with 10ug/ml Dil-ac-LDL for two hours at 37°C followed by staining with DAPI. For matrigel tube formation, endothelial cells were seeded on matrigel-coated 24-well plates ($1x10^5$ cells/well), incubated for one hour at 37°C, and a dded fresh medium. 1-3 days after plating, tube formation was observed.

NIH-PA Author Manuscript

NIH-PA Author Manuscript

NIH-PA Author Manuscript

3D co-cultures and co-transplantation

Amplified LuMECs/LiMECs were used for 3D co-cultures or co-transplantations of AT2 cells and BASCs or dissociated colonies from BASCs. AT2 cells and BASCs were isolated from 7-10 week old mice by FACS sorting using pan-CD45-APC, CD31-APC, Sca1 (Ly-6A/E)-APCCy7, EpCAM-PE-Cy7 with DAPI staining. Freshly isolated cells were mixed with Growth Factor Reduced Matrigel containing LuMECs or LiMECs, and the cell mixtures were plated in transwell plates or transplanted via subcutaneous injection into nude mice. For co-cultures/cotransplantation of individual colonies, similar sized individual colonies were picked under the fluorescence microscope after enzymic digestion. Picked individual colonies were further trypsinized into single cells for qPCR, passaged for subsequent colony formation or transplanted by subcutaneous injection with LuMECs/LiMECs. For “Helper Cell” 3D single cell cultures, freshly isolated EpCAM+ lung epithelial cells were irradiated (26 Grays) and 50,000 cells were resuspended with LuMECs/Matrigel and a single BASC or AT2 cell. For serial passages, Day 14 AT2 cell or BASC 3D co-cultures were dissociated to generate a single-cell suspension followed by FACS for GFP. GFP+ cells were resuspended in fresh LuMEC/Matrigel mixtures. Media for 3D co-cultures were replaced every other day with supplements for up to 14 to 21 days. Mice co-injected with cells/Matrigel were euthanized 4 weeks after injection for analysis of histopathology.

Preparation of TSP1

Blood was collected from 6-8 week old mice by retro-orbital bleeding and centrifuged to separate platelets which were activated by incubation with 1 unit of thrombin for 20 minutes at 37°C. Releasate was then obtained by centrifugatio n to obtain TSP1. Releasate was added to 3D co-culture of BASCs every other day.

Lung injury

In vivo lung injury experiments were conducted in 7-10 week old mice that received naphthalene (275mg/kg) via intraperitoneal injection or bleomycin (0.035U/mice) via intratracheal injection. Conditioned media (CM) was collected from LuMECs/LiMECs which were incubated in serum-free media for 24 hrs following 10-fold concentration. CM was administered via tail vein injection at a volume of 100ul every other day for 21 days after bleomycin injection.

ChIP

ChIP assay was performed with LuMECs/LiMECs that were incubated with serum-free media overnight and were treated with BMP4 (50ng/ml) or BMP4 (50ng/ml) +NOGGIN (100ng/ml) for 30 min. After crosslinking, the sonicated lysate was employed to IP using anti-NFATc1 or anti-mouse IgG with a mix of Protein A/G beads.

Supplementary Material

Refer to Web version on PubMed Central for supplementary material.

Acknowledgments

We thank the BCH FACS facility, members of the Kim Lab, L. Zon, D. Scadden, P. Oh, C. Han, C. Fillmore, K. Townsend, G. Evans and J. Sage for technical assistance and/or helpful discussions, R. Bronson for histopathology. This work was supported by the Hope Funds for Cancer Research (JHL), R01 CA118374 (SR), R01 DK077097 (Y-HT), U01 HL100402 and 1U01HL099997 under NHLBI RFA-HL-09-004 (CFK, BRS, AJW, DS), the Harvard Stem Cell Institute (Y-HT and CFK), the Foundation Leducq (KDB), and RO1 HL090136, American Cancer Society Research Scholar Grant #RSG-08-082-01-MGO, and a Basil O'Conner March of Dimes Starter Award (CFK).

NIH-PA Author Manuscript

NIH-PA Author Manuscript

NIH-PA Author Manuscript

REFERENCES

Adams JC, Lawler J. The thrombospondins. Int J Biochem Cell Biol. 2004; 36:961–968. [PubMed: 15094109]

Aso Y, Yoneda K, Kikkawa Y. Morphologic and biochemical study of pulmonary changes induced by bleomycin in mice. Lab Invest. 1976; 35:558–568. [PubMed: 62893]

Baenziger NL, Brodie GN, Majerus PW. A thrombin-sensitive protein of human platelet membranes. Proc Natl Acad Sci U S A. 1971; 68:240–243. [PubMed: 5276296]

Barkauskas CE, Cronce MJ, Rackley CR, Bowie EJ, Keene DR, Stripp BR, Randell SH, Noble PW, Hogan BL. Type 2 alveolar cells are stem cells in adult lung. J Clin Invest. 2013; 123:3025–3036. [PubMed: 23921127]

Chapman HA, Li X, Alexander JP, Brumwell A, Lorizio W, Tan K, Sonnenberg A, Wei Y, Vu TH. Integrin alpha6beta4 identifies an adult distal lung epithelial population with regenerative potential in mice. J Clin Invest. 2011; 121:2855–2862. [PubMed: 21701069]

Chen H, Herndon ME, Lawler J. The cell biology of thrombospondin-1. Matrix Biol. 2000; 19:597–614. [PubMed: 11102749]

DeLisser HM, Helmke BP, Cao G, Egan PM, Taichman D, Fehrenbach M, Zaman A, Cui Z, Mohan GS, Baldwin HS, et al. Loss of PECAM-1 function impairs alveolarization. J Biol Chem. 2006; 281:8724–8731. [PubMed: 16377626]

Ding BS, Nolan DJ, Guo P, Babazadeh AO, Cao Z, Rosenwaks Z, Crystal RG, Simons M, Sato TN, Worgall S, et al. Endothelial-derived angiocrine signals induce and sustain regenerative lung alveolarization. Cell. 2011; 147:539–553. [PubMed: 22036563]

Dovey JS, Zacharek SJ, Kim CF, Lees JA. Bmi1 is critical for lung tumorigenesis and bronchioalveolar stem cell expansion. Proc Natl Acad Sci U S A. 2008; 105:11857–11862. [PubMed: 18697930]

Ezzie ME, Piper MG, Montague C, Newland CA, Opalek JM, Baran C, Ali N, Brigstock D, Lawler J, Marsh CB. Thrombospondin-1-deficient mice are not protected from bleomycin-induced pulmonary fibrosis. Am J Respir Cell Mol Biol. 2011; 44:556–561. [PubMed: 20581099]

Ganguly P. Isolation and properties of a thrombin-sensitive protein from human blood platelets. J Biol Chem. 1971; 246:4286–4290. [PubMed: 4103788]

Giangreco A, Reynolds SD, Stripp BR. Terminal bronchioles harbor a unique airway stem cell population that localizes to the bronchoalveolar duct junction. Am J Pathol. 2002; 161:173–182. [PubMed: 12107102]

Green MD, Chen A, Nostro MC, d'Souza SL, Schaniel C, Lemischka IR, Gouon-Evans V, Keller G, Snoeck HW. Generation of anterior foregut endoderm from human embryonic and induced pluripotent stem cells. Nat Biotechnol. 2011; 29:267–272. [PubMed: 21358635]

Hesser BA, Liang XH, Camenisch G, Yang S, Lewin DA, Scheller R, Ferrara N, Gerber HP. Down syndrome critical region protein 1 (DSCR1), a novel VEGF target gene that regulates expression of inflammatory markers on activated endothelial cells. Blood. 2004; 104:149–158. [PubMed: 15016650]

Horsley V, Aliprantis AO, Polak L, Glimcher LH, Fuchs E. NFATc1 balances quiescence and proliferation of skin stem cells. Cell. 2008; 132:299–310. [PubMed: 18243104]

Iruela-Arispe ML, Liska DJ, Sage EH, Bornstein P. Differential expression of thrombospondin 1, 2, and 3 during murine development. Dev Dyn. 1993; 197:40–56. [PubMed: 8400410]

Jakkula M, Le Cras TD, Gebb S, Hirth KP, Tuder RM, Voelkel NF, Abman SH. Inhibition of angiogenesis decreases alveolarization in the developing rat lung. Am J Physiol Lung Cell Mol Physiol. 2000; 279:L600–607. [PubMed: 10956636]

Jones DL, Wagers AJ. No place like home: anatomy and function of the stem cell niche. Nat Rev Mol Cell Biol. 2008; 9:11–21. [PubMed: 18097443]

Kim CF. Paving the road for lung stem cell biology: bronchioalveolar stem cells and other putative distal lung stem cells. Am J Physiol Lung Cell Mol Physiol. 2007; 293:L1092–1098. [PubMed: 17693488]

NIH-PA Author Manuscript NIH-PA Author Manuscript NIH-PA Author Manuscript

Kim CF, Jackson EL, Woolfenden AE, Lawrence S, Babar I, Vogel S, Crowley D, Bronson RT, Jacks T. Identification of bronchioalveolar stem cells in normal lung and lung cancer. Cell. 2005; 121:823–835. [PubMed: 15960971]

Lawler J. Thrombospondin-1 as an endogenous inhibitor of angiogenesis and tumor growth. J Cell Mol Med. 2002; 6:1–12. [PubMed: 12003665]

Lawler J, Sunday M, Thibert V, Duquette M, George EL, Rayburn H, Hynes RO. Thrombospondin-1 is required for normal murine pulmonary homeostasis and its absence causes pneumonia. J Clin Invest. 1998; 101:982–992. [PubMed: 9486968]

Lawler JW, Slayter HS, Coligan JE. Isolation and characterization of a high molecular weight glycoprotein from human blood platelets. J Biol Chem. 1978; 253:8609–8616. [PubMed: 101549]

Lee JH, Kim J, Gludish D, Roach RR, Saunders AH, Barrios J, Woo AJ, Chen H, Conner DA, Fujiwara Y, et al. Surfactant protein-C chromatin- bound green fluorescence protein reporter mice reveal heterogeneity of surfactant protein C-expressing lung cells. Am J Respir Cell Mol Biol. 2013; 48:288–298. [PubMed: 23204392]

Longmire TA, Ikonomou L, Hawkins F, Christodoulou C, Cao Y, Jean JC, Kwok LW, Mou H, Rajagopal J, Shen SS, et al. Efficient derivation of purified lung and thyroid progenitors from embryonic stem cells. Cell Stem Cell. 2012; 10:398–411. [PubMed: 22482505]

Maloney JP, Stearman RS, Bull TM, Calabrese DW, Tripp-Addison ML, Wick MJ, Broeckel U, Robbins IM, Wheeler LA, Cogan JD, et al. Loss-of-function thrombospondin-1 mutations in familial pulmonary hypertension. Am J Physiol Lung Cell Mol Physiol. 2012; 302:L541–554. [PubMed: 22198906]

Masterson JC, Molloy EL, Gilbert JL, McCormack N, Adams A, O'Dea S. Bone morphogenetic protein signalling in airway epithelial cells during regeneration. Cell Signal. 2011; 23:398–406. [PubMed: 20959141]

McQualter JL, Yuen K, Williams B, Bertoncello I. Evidence of an epithelial stem/progenitor cell hierarchy in the adult mouse lung. Proc Natl Acad Sci U S A. 2010; 107:1414–1419. [PubMed: 20080639]

Minami T, Horiuchi K, Miura M, Abid MR, Takabe W, Noguchi N, Kohro T, Ge X, Aburatani H, Hamakubo T, et al. Vascular endothelial growth factor- and thrombin-induced termination factor, Down syndrome critical region-1, attenuates endothelial cell proliferation and angiogenesis. J Biol Chem. 2004; 279:50537–50554. [PubMed: 15448146]

Morrison SJ, Spradling AC. Stem cells and niches: mechanisms that promote stem cell maintenance throughout life. Cell. 2008; 132:598–611. [PubMed: 18295578]

Mou H, Zhao R, Sherwood R, Ahfeldt T, Lapey A, Wain J, Sicilian L, Izvolsky K, Musunuru K, Cowan C, et al. Generation of multipotent lung and airway progenitors from mouse ESCs and patient-specific cystic fibrosis iPSCs. Cell Stem Cell. 2012; 10:385–397. [PubMed: 22482504]

Nolan DJ, Ginsberg M, Israely E, Palikuqi B, Poulos MG, James D, Ding BS, Schachterle W, Liu Y, Rosenwaks Z, et al. Molecular signatures of tissue- specific microvascular endothelial cell heterogeneity in organ maintenance and regeneration. Dev Cell. 2013; 26:204–219. [PubMed: 23871589]

O'Shea KS, Dixit VM. Unique distribution of the extracellular matrix component thrombospondin in the developing mouse embryo. J Cell Biol. 1988; 107:2737–2748. [PubMed: 3204123]

Otto WR. Lung epithelial stem cells. J Pathol. 2002; 197:527–535. [PubMed: 12115868]

Rawlins EL, Okubo T, Xue Y, Brass DM, Auten RL, Hasegawa H, Wang F, Hogan BL. The role of Scgb1a1+ Clara cells in the long-term maintenance and repair of lung airway, but not alveolar, epithelium. Cell Stem Cell. 2009; 4:525–534. [PubMed: 19497281]

Rock JR, Barkauskas CE, Cronce MJ, Xue Y, Harris JR, Liang J, Noble PW, Hogan BL. Multiple stromal populations contribute to pulmonary fibrosis without evidence for epithelial to mesenchymal transition. Proc Natl Acad Sci U S A. 2011; 108:E1475–1483. [PubMed: 22123957]

Rock JR, Onaitis MW, Rawlins EL, Lu Y, Clark CP, Xue Y, Randell SH, Hogan BL. Basal cells as stem cells of the mouse trachea and human airway epithelium. Proc Natl Acad Sci U S A. 2009; 106:12771–12775. [PubMed: 19625615]

NIH-PA Author Manuscript

NIH-PA Author Manuscript

NIH-PA Author Manuscript

Rosendahl A, Pardali E, Speletas M, Ten Dijke P, Heldin CH, Sideras P. Activation of bone morphogenetic protein/Smad signaling in bronchial epithelial cells during airway inflammation. Am J Respir Cell Mol Biol. 2002; 27:160–169. [PubMed: 12151307]

Ryeom S, Baek KH, Rioth MJ, Lynch RC, Zaslavsky A, Birsner A, Yoon SS, McKeon F. Targeted deletion of the calcineurin inhibitor DSCR1 suppresses tumor growth. Cancer Cell. 2008; 13:420–431. [PubMed: 18455125]

Sountoulidis A, Stavropoulos A, Giaglis S, Apostolou E, Monteiro R, Chuva de Sousa Lopes SM, Chen H, Stripp BR, Mummery C, Andreakos E, et al. Activation of the canonical Bone Morphogenetic Protein (BMP) pathway during lung morphogenesis and adult lung tissue repair. PLoS One. 2012; 7:e41460. [PubMed: 22916109]

Teisanu RM, Chen H, Matsumoto K, McQualter JL, Potts E, Foster WM, Bertoncello I, Stripp BR. Functional analysis of two distinct bronchiolar progenitors during lung injury and repair. Am J Respir Cell Mol Biol. 2011; 44:794–803. [PubMed: 20656948]

Tropea KA, Leder E, Aslam M, Lau AN, Raiser DM, Lee JH, Balasubramaniam V, Fredenburgh LE, Alex Mitsialis S, Kourembanas S, et al. Bronchioalveolar stem cells increase after mesenchymal stromal cell treatment in a mouse model of bronchopulmonary dysplasia. Am J Physiol Lung Cell Mol Physiol. 2012; 302:L829–837. [PubMed: 22328358]

Vintersten K, Monetti C, Gertsenstein M, Zhang P, Laszlo L, Biechele S, Nagy A. Mouse in red: red fluorescent protein expression in mouse ES cells, embryos, and adult animals. Genesis. 2004; 40:241–246. [PubMed: 15593332]

Wright DE, Cheshier SH, Wagers AJ, Randall TD, Christensen JL, Weissman IL. Cyclophosphamide/granulocyte colony-stimulating factor causes selective mobilization of bone marrow hematopoietic stem cells into the blood after M phase of the cell cycle. Blood. 2001; 97:2278–2285. [PubMed: 11290588]

Zacharek SJ, Fillmore CM, Lau AN, Gludish DW, Chou A, Ho JW, Zamponi R, Gazit R, Bock C, Jager N, et al. Lung stem cell self-renewal relies on BMI1-dependent control of expression at imprinted loci. Cell Stem Cell. 2011; 9:272–281. [PubMed: 21885022]

Zhang Y, Goss AM, Cohen ED, Kadzik R, Lepore JJ, Muthukumaraswamy K, Yang J, DeMayo FJ, Whitsett JA, Parmacek MS, et al. A Gata6-Wnt pathway required for epithelial stem cell development and airway regeneration. Nat Genet. 2008; 40:862–870. [PubMed: 18536717]

NIH-PA Author Manuscript

NIH-PA Author Manuscript

NIH-PA Author Manuscript

HIGHLIGHTS

- Lung endothelial cells control lung stem cell differentiation
- In vitro expansion and multi-lineage differentiation of single lung stem cells
- Endothelial TSP1 is required for alveolar differentiation and lung regeneration
- BMP4 induces lung-specific, calcineurin/NFATc1-dependent TSP1 expression

NIH-PA Author Manuscript
NIH-PA Author Manuscript
NIH-PA Author Manuscript

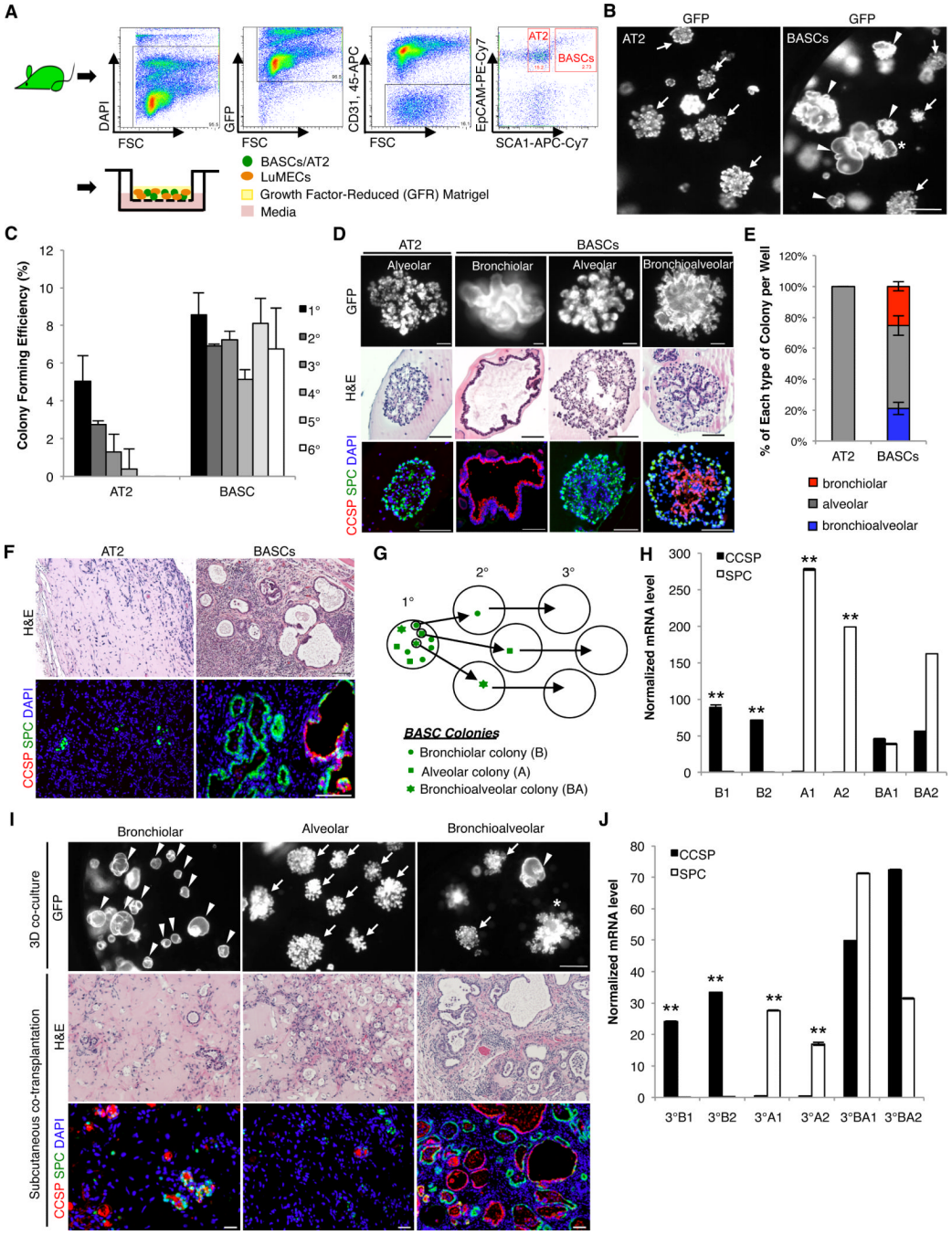

Figure 1. LuMECs support BASC self-renewal and differentiation in vitro and in vivo

(A) Schematic of FACS strategy to enrich for AT2 cells and BASCs from β-actin-GFP mice and 3D co-culture with LuMECs. CD45+ hematopoietic and CD31+ endothelial cells were excluded. EpCAM+ epithelial cells were selected. From these selections, Sca1-positive cells were BASCs and Sca1-negative cells were AT2 cells. (B) Representative images of GFP fluorescent colonies from 3D co-culture of AT2 cells (left) or BASCs (right) with LuMECs after 14 days. Arrowhead, bronchiolar colony; arrow, alveolar colony; asterisk, bronchioalveolar colony. Scale bar, 500um. (C) Self-renewal of AT2 cells and BASCs in 3D LuMEC co-cultures. Primary colonies (1°) were dissociated a nd GFP+ cells were replated for secondary (2°) and subsequent (3°, 4°, 5°, 6°) colony formati on. Colony forming

NIH-PA Author Manuscript

NIH-PA Author Manuscript

NIH-PA Author Manuscript

efficiency: number of colonies formed/number of cells plated per well as a percentage. Data presented are the mean of three independent experiments with triplicate wells. Error bars indicate standard deviation. (D) Representative GFP images of alveolar colonies from AT2 cells (top, left) and bronchiolar, alveolar, and bronchioalveolar colonies from BASCs (top, right). H&E (middle) and IF (bottom) for CCSP (red), SPC (green), and DAPI (blue) show BASC differentiation into club (Clara) cells and AT2 cells. Scale bar, 100um. (E) Quantification of each colony type from AT2 cell (n=687) or BASC co-cultures (n=842). 25.4% of colonies were bronchiolar, 53.5% were alveolar, and 21.1% were mixed. The mean percentage of total colonies per well represented by each type of colony is shown. n=number of colonies scored. Data presented are the mean of seven independent experiments with triplicate wells. Error bars indicate standard deviation.
(F) Subcutaneous co-transplantation of AT2 cells or BASCs mixed with LuMEC/Matrigel. H&E (top) and IF (bottom) for CCSP (red), SPC (green), and DAPI (blue) show that only BASCs co-injected with LuMECs formed epithelial structures with cells positive for CCSP, SPC, or both; BASCs, n=7/8 mice injected formed epithelial structures; AT2 cells, n=9/9 mice injected did not yield epithelial structures. Images are representative of three independent experiments. Scale bar, 100um. (G) Schematic of clonal serial passage analysis. 1° colonies were plated for 2° or 3° colony formation (I) and half of the cells were used for qPCR (H and J). Data shown are from 20 individual colonies per type analyzed over four independent experiments. (H) Representative qPCR analysis validating expression of SPC (white bars) and CCSP (black bars) in cells from two different individual colonies. B1, B2: primary bronchiolar colony; A1, A2: primary alveolar colony; BA1, BA2: primary bronchioalveolar colony. Normalized to *Gapdh*. Data presented are the mean of triplicate wells. Error bars indicate standard deviation (**, $p<0.001$). (I) Representative GFP images of 2° colo nies from passage of each colony type. Arrowhead, bronchiolar colony; arrow, alveolar colony; asterisk, bronchioalveolar colony. Scale bar, 500um (top); H&E (middle) and IF (bottom) analysis for CCSP (red), SPC (green), and DAPI (blue) in tissue sections from subcutaneous transplantation of cells from BASC-derived bronchiolar (left)(n=3/8 mice formed epithelial structures), alveolar (middle)(n=15/15 mice did not yield epithelial structures), or bronchioalveolar colonies (right)(n=9/9 mice generated epithelial structures). Scale, 100um. (J) Representative qPCR analysis in tertiary colonies as in H. 3°B1, 3°B2: tertiary bronchiolar colony; 3°A1, 3°A2: tertiary alveolar colony; 3°BA1, 3°BA2: tertiary bronchioalveolar colony. N ormalized to *Gapdh*. Data presented are the mean of triplicate wells. Error bars indicate standard deviation (**, $p<0.001$). See also Figure S1.

NIH-PA Author Manuscript

NIH-PA Author Manuscript

NIH-PA Author Manuscript

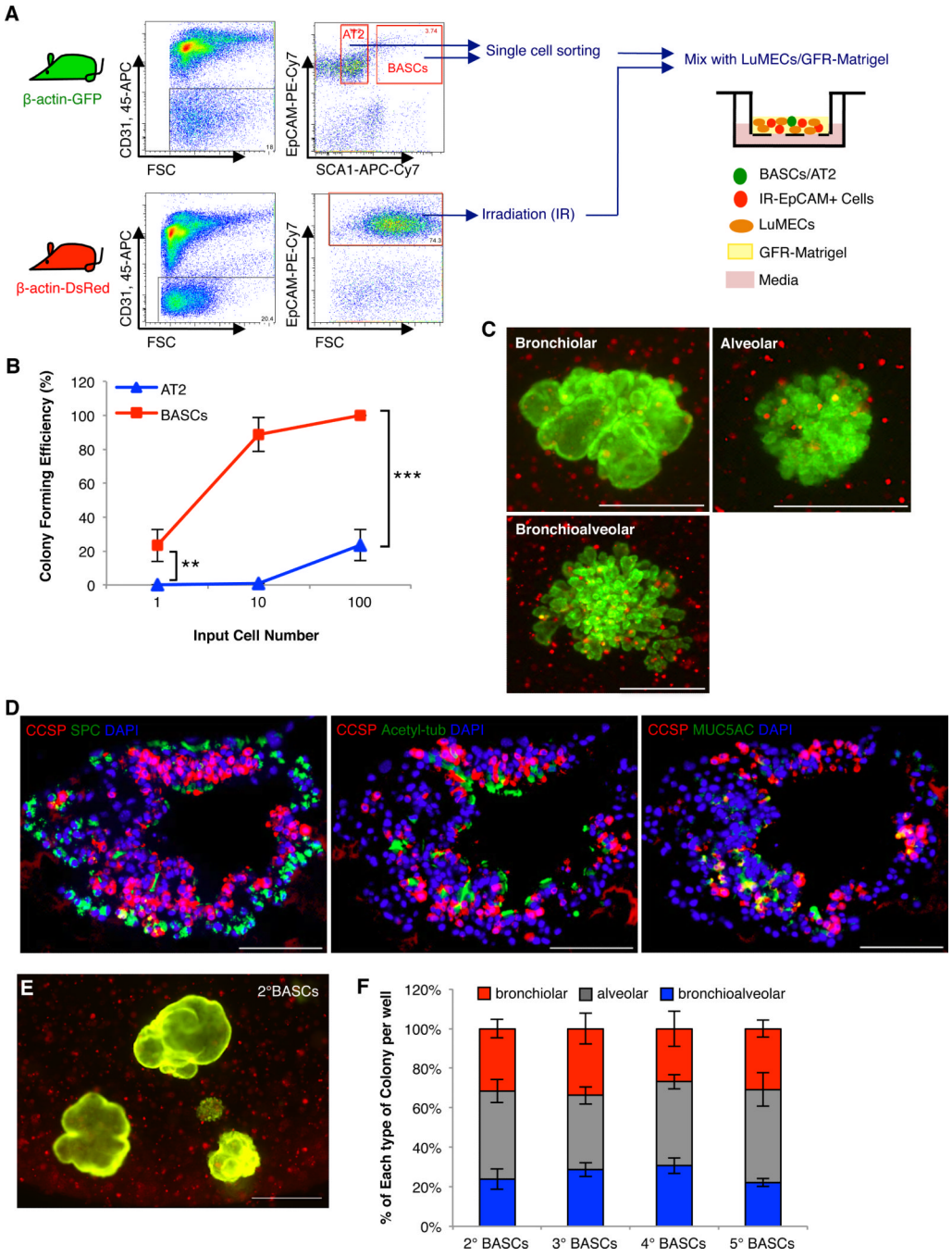

Figure 2. Single BASCs develop multi-lineage lung organoids

(A) Schematic of "helper cell" 3D co-cultures. Single GFP+ BASCs were mixed with irradiated EpCAM+ DsRed lung epithelial cells and co-cultured with LuMECs. (B) Limiting dilution assay in helper cell 3D co-cultures. The percentage of wells with colony formation from 1, 10, or 100 GFP+ cells for each population (BASCs, red; AT2, blue) is shown. n=180, 105, and 90 wells with 1, 10 or 100 cells plated, respectively. Data presented are the mean of four independent experiments with multiplicate wells. Error bars indicate standard deviation (**, p<0.001; ***, p<0.0001). (C) Representative merged fluorescent images (GFP, DsRed) from single GFP+ BASC helper cell co-cultures. Scale bar, 500um. (D) Representative IF in a bronchioalveolar colony derived from a single BASC; CCSP (red),

NIH-PA Author Manuscript

NIH-PA Author Manuscript

NIH-PA Author Manuscript

SPC (green), and DAPI (blue) (top); CCSP (red), Acetylated-tubulin (green), and DAPI (blue) (middle); CCSP (red), MUC5AC (green), and DAPI (blue) (bottom). Scale bar, 100um. (E) Representative merged image (GFP, DsRed) of single BASC-derived secondary colonies. Scale bar, 500um. (F) Quantification of colony types from single BASC-derived bronchioalveolar colonies (n=14 bronchioalveolar colonies tested, n=384 secondary colonies (2°BASCs) scored) or from subsequent serial passage (n=475 3°BASCs, n=465 4°BASCs, n=452 5°BASCs). n= number of colonies scored. Data presented are the mean of three independent experiments with four individual colonies. Error bars indicate standard deviation.

NIH-PA Author Manuscript
NIH-PA Author Manuscript
NIH-PA Author Manuscript

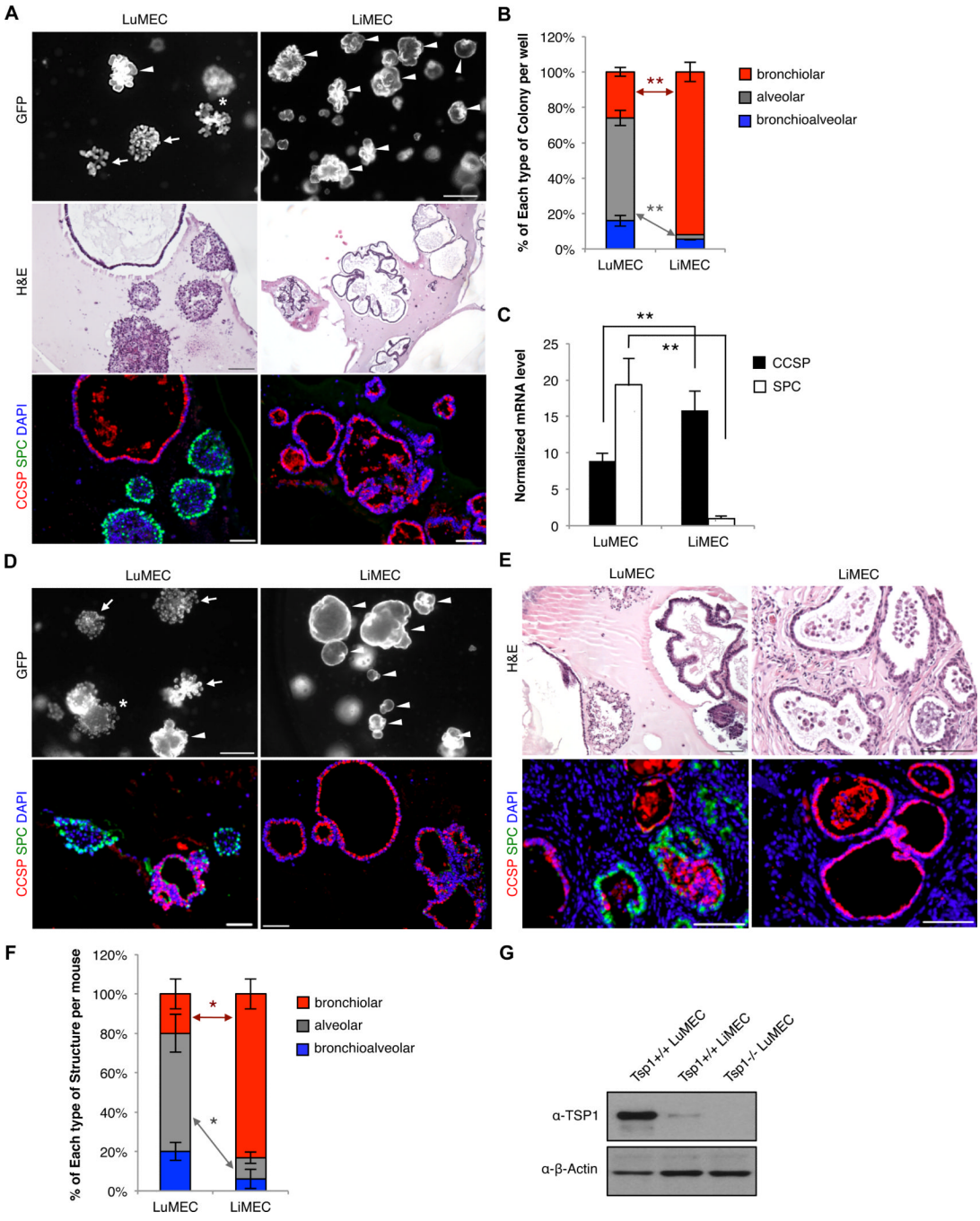

Figure 3. Organ-specific endothelial effects on BASC differentiation

(A) Representative images from BASCs co-cultured with lung endothelial cells (LuMECs) or liver endothelial cells (LiMECs). Arrowhead, bronchiolar colony; arrow, alveolar colony; asterisk, bronchioalveolar colony. Scale bar, 500um (top); H&E (middle); IF (bottom) for CCSP (red), SPC (green), and DAPI (blue). Scale bar, 100um. (B) Quantification of colony types from LuMEC or LiMEC co-cultures with; BASC/LiMEC co-cultures yielded 3.5-fold increased bronchiolar and 21.5-fold diminished alveolar colony yield per well compared to BASC/LuMEC cultures ($p<0.001$) (LuMECs, n=663 colonies; LiMECs, n=627). n=number of colonies scored. Data presented are the mean of five independent experiments with triplicate wells. Error bars indicate standard deviation (**, $p<0.001$). (C) qPCR for CCSP

NIH-PA Author Manuscript

NIH-PA Author Manuscript

NIH-PA Author Manuscript

(black bars) and SPC (white bars) from co-cultures; 1.8-fold greater CCSP expression and 19.3-fold less SPC expression in BASC/LiMEC cultures relative to BASC/LuMEC ($p<0.001$). Normalized to *Gapdh*. Data presented are the mean of three independent experiments with triplicate wells. Error bars indicate standard deviation (**, $p<0.001$). (D) Representative results from BASC/LuMEC bronchioalveolar colonies passaged for co-culture with LuMECs or LiMECs. GFP fluorescent images (top) and IF analysis (bottom) for CCSP (red), SPC (green), and DAPI (blue). Arrowhead, bronchiolar colony; arrow, alveolar colony; asterisk, bronchioalveolar colony. Scale bar, 500um in top, 100um in bottom. (E) H&E (top) and IF (bottom) analysis for CCSP (red), SPC (green), and DAPI (blue) in tissue sections from subcutaneous co-injection of cells from BASC/LuMEC bronchioalveolar colonies co-transplanted with LuMECs or LiMECs. Scale bar, 100um. (F) Quantitative analysis of epithelial structures from (E). Data presented are the mean of two independent experiments with two individual mice wells. Error bars indicate standard deviation (*, $p<0.01$). (G) Immunoblotting for TSP1 in LuMECs and LiMECs. *Tsp1*−/−LuMECs was used for negative control. β-actin loading control. See also Figure S2.

NIH-PA Author Manuscript
NIH-PA Author Manuscript
NIH-PA Author Manuscript

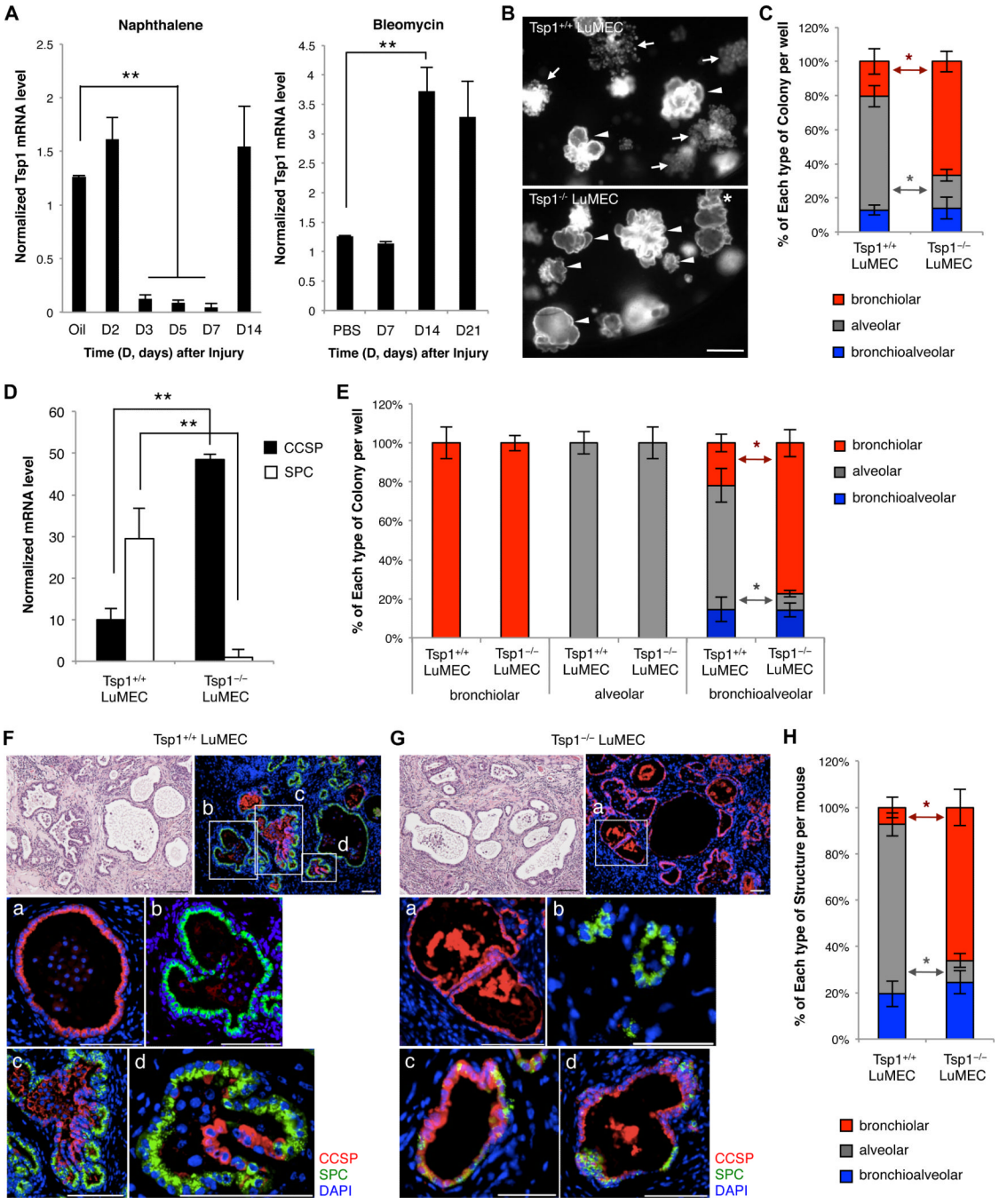

Figure 4. *Tsp1* deficiency in LuMECs inhibits alveolar differentiation in vitro and in vivo

(A) qPCR for *Tsp1* in LuMECs isolated at time points (D, days) after naphthalene (left) or bleomycin (right) injury. Corn oil or PBS, diluent controls for naphthalene or bleomycin, respectively. *Tsp1* levels were 10.1-fold less than control during naphthalene injury repair and 2.9-fold higher than control during bleomycin injury repair ($p<0.001$). Normalized to *Gapdh*. Data presented are the mean of samples from three individual mice. Error bars indicate standard deviation (**, $p<0.001$). (B) Representative GFP images of BASCs co-cultured with $Tsp1^{+/+}$ (top) or $Tsp1^{-/-}$ LuMECs (bottom). Arrowhead, bronchiolar colony; arrow, alveolar colony; asterisk, bronchioalveolar colony. Scale bar, 500um. (C) Quantification of colony types from BASCs co-cultured with $Tsp1^{+/+}$ or $Tsp1^{-/-}$ LuMECs

NIH-PA Author Manuscript

NIH-PA Author Manuscript

NIH-PA Author Manuscript

(n=605, 753, respectively). n=number of colonies scored. Data presented are the mean of five independent experiments with triplicate wells. Error bars indicate standard deviation (*, p<0.01). (D) qPCR analysis for SPC and CCSP from colonies as in B; 4.8-fold higher levels of CCSP expression and 29.5-fold less SPC expression in BASC/*Tsp1*$^{-/-}$ LuMEC co-cultures vs BASC/*Tsp1*$^{+/+}$ LuMECs (p<0.001). Normalized to *Gapdh*. Data presented are the mean of three independent experiments with triplicate wells. Error bars indicate standard deviation (**, p<0.001). (E) Quantification of colony types from passaged colonies co-cultured with *Tsp1*$^{+/+}$ or *Tsp1*$^{-/-}$ LuMECs (Bronchiolar: n=471, *Tsp1*$^{+/+}$; n=633, *Tsp1*$^{-/-}$. Alveolar: n=460, *Tsp1*$^{+/+}$; n=532, *Tsp1*$^{-/-}$. Bronchioalveolar: n=566, *Tsp1*$^{+/+}$; n=651, *Tsp1*$^{-/-}$). Cells from bronchioalveolar colonies co-cultured with *Tsp1*$^{-/-}$ LuMECs produced 3.6-fold more bronchiolar colonies and 5.7-fold less alveolar colonies (p<0.01), respectively, than co-cultures with *Tsp1*$^{+/+}$ LuMECs. n=number of colonies scored. Data presented are the mean of four independent experiments with duplicate wells of five individual colonies. Error bars indicate standard deviation (*, p<0.01) (F-G) H&E (top left) and IF analysis for CCSP (red), SPC (green), and DAPI (blue) in tissue sections from subcutaneous co-injection of bronchioalveolar colonies with *Tsp1*$^{+/+}$ (F) or *Tsp1*$^{-/-}$ LuMECs (G). Insets (top right) show high-power view (a, bronchiolar; b, alveolar; c, d, bronchioalveolar). Scale bar, 100um. (H) Quantitative analysis of epithelial structures from (F and G). Data presented are the mean of two independent experiments with three individual mice. Error bars indicate standard deviation (*, p<0.01). See also Figure S3.

NIH-PA Author Manuscript
NIH-PA Author Manuscript
NIH-PA Author Manuscript

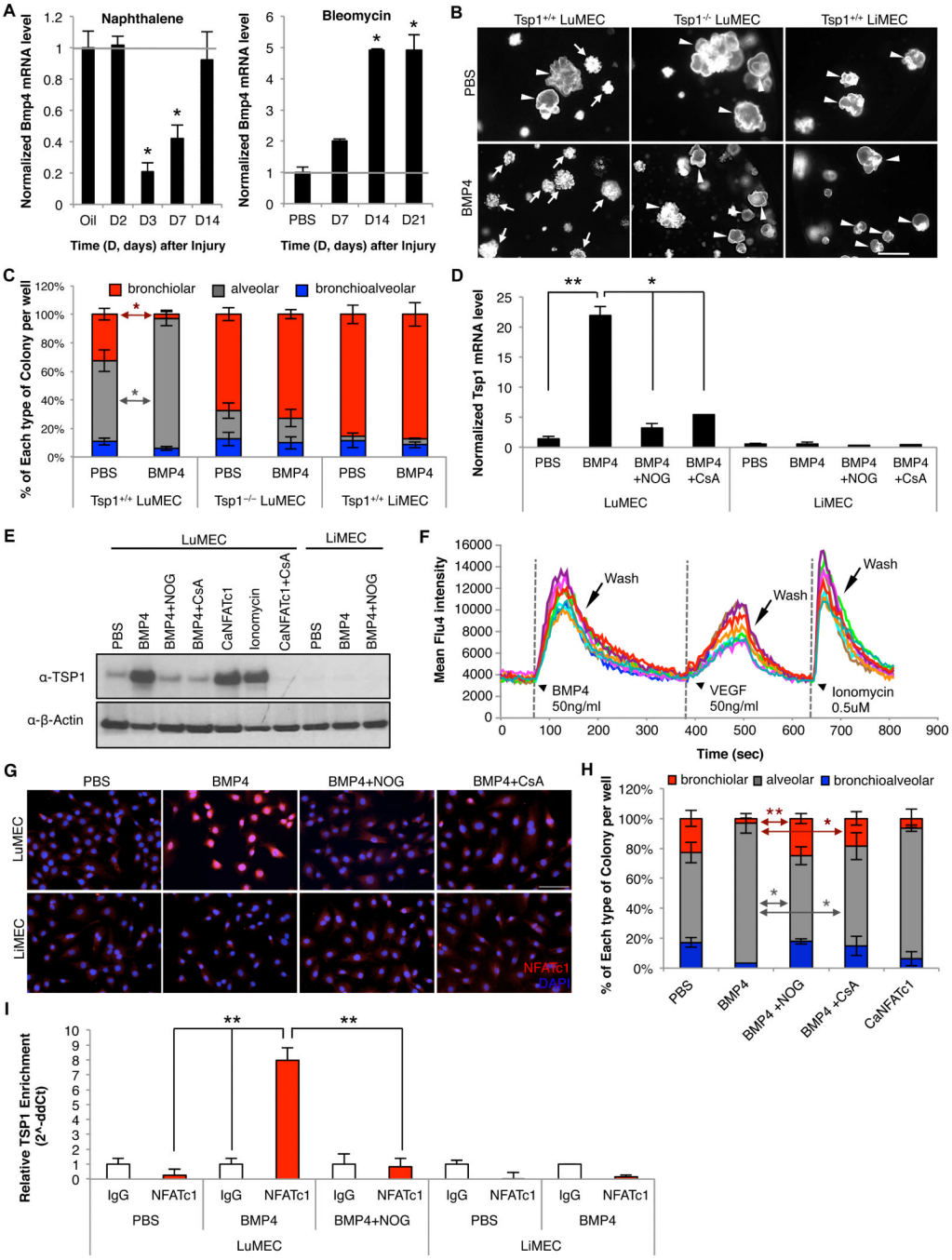

Figure 5. BMP4-induced, NFATc1-dependent *Tsp1* expression in LuMECs is required for BASC alveolar differentiation

(A) qPCR for *Bmp4* from LuMECs isolated at time points (D, days) after naphthalene (left) or bleomycin (right) injury. Normalized to *Gapdh* and expression in controls is set to 1 for comparison. Data presented are the mean of samples from three individual mice. Error bars indicate standard deviation (*, p<0.01). (B) Representative GFP images of BASC co-cultures treated with PBS or BMP4 (50ng/ml). BASC 3D co-cultures with *Tsp1*$^{+/+}$ LuMEC (left), *Tsp1*$^{-/-}$ LuMEC (middle), or LiMEC (right) are shown. Arrowhead, bronchiolar colony; arrow, alveolar colony. Scale bar, 500um. (C) Quantification of colony types from BASC co-cultures treated with PBS or BMP4 with *Tsp1*$^{+/+}$ LuMEC (n=414, PBS; n=367,

NIH-PA Author Manuscript

NIH-PA Author Manuscript

NIH-PA Author Manuscript

BMP4), *Tsp1*$^{-/-}$ LuMEC (n=498, PBS; n=425, BMP4), or *Tsp1*$^{+/+}$ LiMEC (n=376, PBS; n=334, BMP4). BASC/*Tsp1*$^{+/+}$ LuMEC co-cultures with BMP4 treatment showed 1.6-fold more alveolar colonies than PBS control ($p<0.01$) and 3.0-fold less bronchiolar colonies than control ($p<0.01$). n=number of colonies scored. Data presented are the mean of three independent experiments with triplicate wells. Error bars indicate standard deviation (*, $p<0.01$). (D) qPCR for *Tsp1* in LuMECs isolated by FACS (GFP-negative) after co-culture with BASCs in the presence of PBS control, BMP4, BMP4 plus Noggin (NOG) or BMP4 plus cyclosporin A (CsA). BMP4 treatment increased *Tsp1* levels in LuMECs by 15.5-fold greater than PBS control ($p<0.001$). Normalized to *Gapdh*. Data presented are the mean of three independent experiments with triplicate wells. Error bars indicate standard deviation (*, $p<0.01$; **, $p<0.001$). (E) Immunoblotting for TSP1 in LuMECs treated as indicated. CaNFATc1, LuMEC infected with constitutively active form of NFATc1. β-actin loading control. (F) Intracellular calcium measurement. BMP4, VEGF, or ionomycin was loaded at indicated time (arrow head) followed by washing (arrow). Induced calcium mobilization was monitored by flou-4. (G) IF analysis for NFATc1 (red) and DAPI (blue) in LuMEC cultures treated as in E. Scale bar, 100um. (H) Quantification of colony types from passage of BASC/LuMEC bronchioalveolar colonies treated with PBS (n=415), BMP4 (n=385), BMP4 plus NOG (n=371), or BMP4 plus CsA (n=392) or co-cultured with CaNFATc1-LuMECs (n=388). Alveolar colony formation was 1.6-fold less in BMP4-treated cultures with NOG ($p<0.01$) and 1.4-fold less with CsA ($p<0.01$). Bronchiolar colony formation with BMP4 was increased 7.8-fold ($p<0.001$) with NOG and 5.6-fold greater after CsA ($p<0.01$). BASC/ CaNFATc1-LuMEC co-cultures formed 1.5-fold more alveolar colonies ($p<0.01$) and 3.5-fold less bronchiolar colonies ($p<0.001$) compared to BASC/LuMEC. n=number of colonies scored. Data presented are the mean of three independent experiments with five individual colonies. Error bars indicate standard deviation (*, $p<0.01$; **, $p<0.001$). (I) qPCR using *Tsp1* promoter primers and DNA purified from NFATc1-ChIP in LuMECs after treatments indicated for 30min. NFATc1 ChIP in LuMECs with BMP4 addition showed 8-fold greater *Tsp1* enrichment than IgG control and 30.8-fold greater than PBS control, $p<0.001$. The enrichment relative to *Gapdh* is shown. Data presented are the mean of three independent experiments with triplicate wells. Error bars indicate standard error of mean (**, $p<0.001$). See also Figure S4.

NIH-PA Author Manuscript
NIH-PA Author Manuscript
NIH-PA Author Manuscript

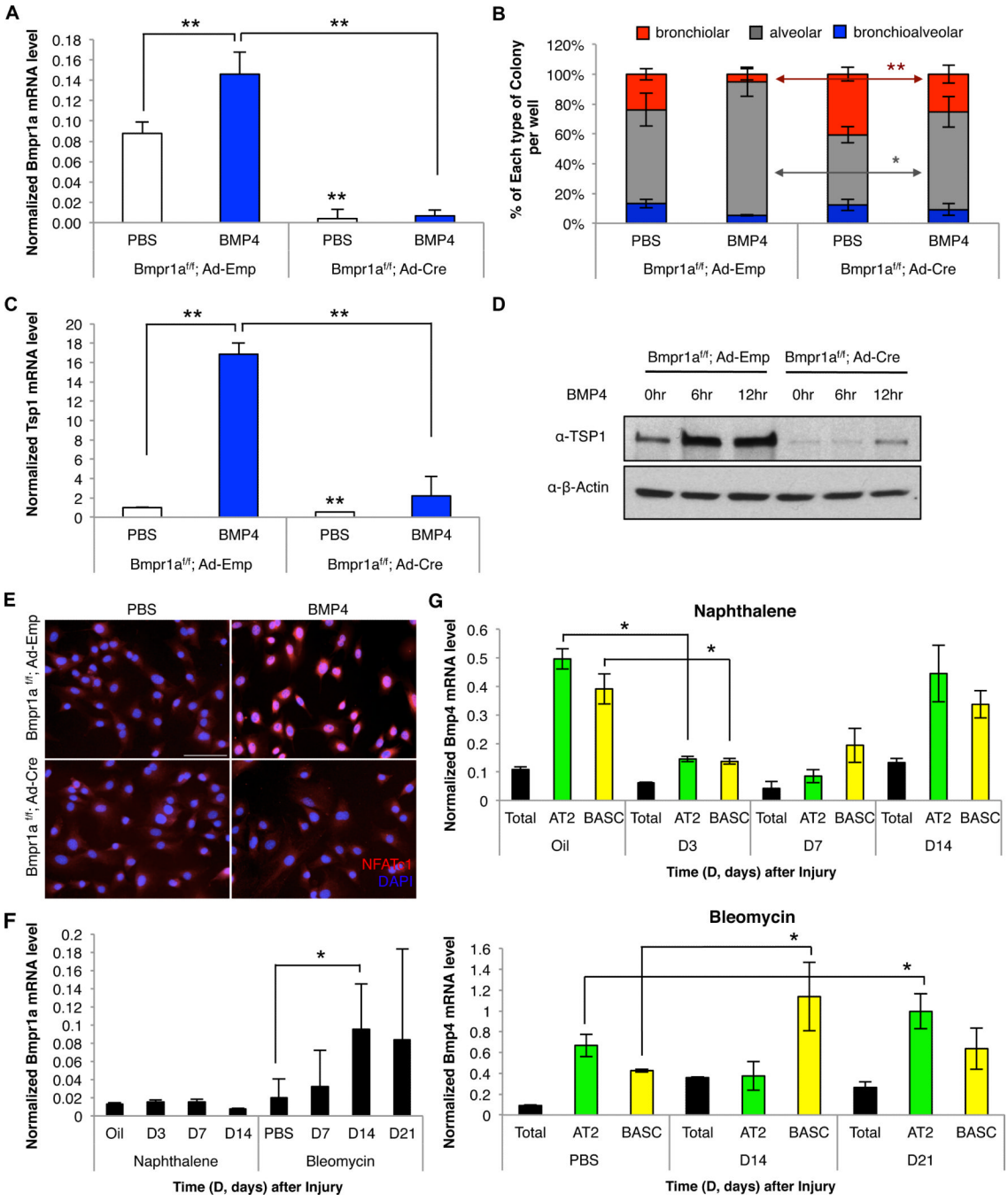

Figure 6. Bmpr1a is required for BASC alveolar differentiation

(A) qPCR for *Bmpr1a* in *Bmpr1a*$^{f/f}$; Ad-Emp (Ad-Emp) or *Bmpr1a*$^{f/f}$; Ad-Cre (Ad-Cre) LuMECs isolated from co-culture with BASCs with (blue bars) or without BMP4 (white bars). Normalized to *Gapdh*. Data presented are the mean of three independent experiments with triplicate wells. Error bars indicate standard deviation (**, p<0.001). (B) Quantification of colony types from BASC co-cultures treated with PBS or BMP4 with Ad-Emp LuMECs (n=423, PBS; n=388, BMP4) or Ad-Cre LuMECs (n=456, PBS; n=441, BMP4). After BMP4 treatment, whereas BASC/Ad-Emp LuMEC generated 3.8-fold less bronchiolar colonies (p<0.001) and 1.4-fold more alveolar colonies (p<0.01) compared to PBS controls, BASC/Ad-Cre LuMEC produced bronchiolar and alveolar colonies comparable to PBS

NIH-PA Author Manuscript

NIH-PA Author Manuscript

NIH-PA Author Manuscript

controls. n=number of colonies scored. Data presented are the mean of three independent experiments with triplicate wells. Error bars indicate standard deviation (*, $p<0.01$; **, $p<0.001$). (C) qPCR for *Tsp1* as in A. (D) Immunoblotting for TSP1 in *Bmpr1a*$^{f/f}$; Ad-Emp or *Bmpr1a*$^{f/f}$; Ad-Cre LuMECs at indicated time points after BMP4 treatment. β-actin loading control. (E) IF analysis for NFATc1 (red) and DAPI (blue) in Ad-Emp or Ad-Cre LuMEC cultures treated with PBS or BMP4. Scale bar, 100um. (F-G) qPCR for *Bmpr1a* (black bars) from LuMECs (F) or *Bmp4* from AT2 cells (green bars), BASCs (yellow bars) or total live lung cells (black bars) (G) isolated at indicated time points after naphthalene (G, top) or bleomycin (G, bottom). Normalized to *Gapdh*. Data presented are the mean of samples from three independent mice. Error bars indicate standard deviation (*, $p<0.01$). See also Figure S5.

NIH-PA Author Manuscript

NIH-PA Author Manuscript

NIH-PA Author Manuscript

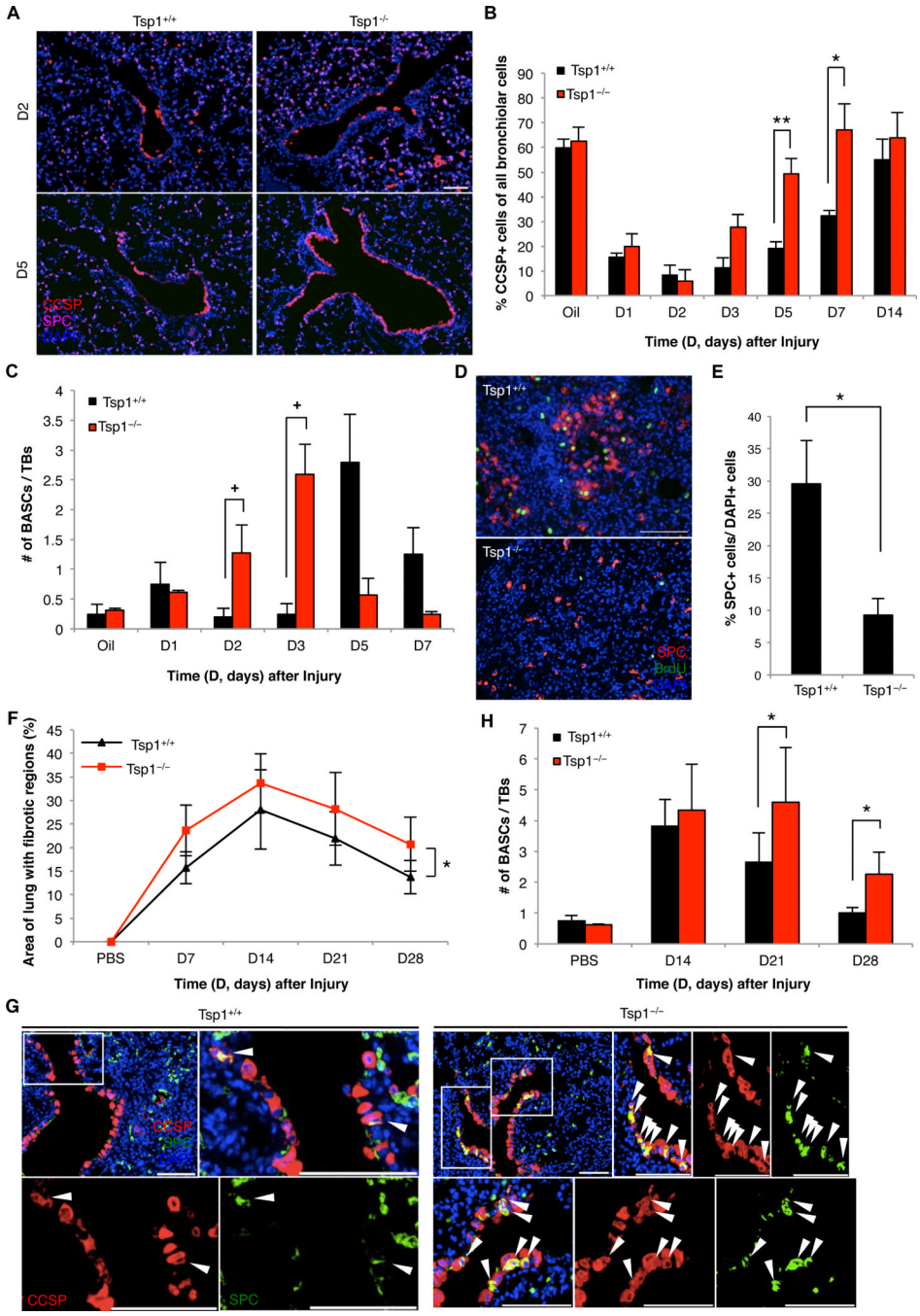

Figure 7. Accelerated bronchiolar injury repair and impaired alveolar injury repair in *Tsp1*-null mice

(A) Representative images showing club cell injury or repair determined by IF for CCSP (red), SPC (purple), and DAPI (blue) in lung tissue sections from *Tsp1*$^{+/+}$ and *Tsp1*$^{-/-}$ mice at 2 days (top) or 5 days (bottom) after naphthalene. (B-C) Quantification of naphthalene injury repair in *Tsp1*$^{+/+}$ (black bars) and *Tsp1*$^{-/-}$ (red bars) lungs. (B) For club cells, the percentage of DAPI-positive, CCSP-positive bronchiolar cells was assessed at indicated time points (*, $p<0.01$; **, $p<0.001$). (C) The numbers of CCSP-positive, SPC-positive BASCs in terminal bronchioles (TBs) were counted at indicated time points (+, $p<0.05$). (D) Representative IF analysis for SPC (red), BrdU (green), and DAPI (blue) in fibrotic lung

NIH-PA Author Manuscript

NIH-PA Author Manuscript

NIH-PA Author Manuscript

regions from *Tsp1*$^{+/+}$ or *Tsp1*$^{-/-}$ mice 21 days post intratracheal bleomycin injection. (E-F) Quantification of bleomycin injury repair. (E) The percentage of DAPI-positive, SPC-positive cells 21 days after bleomycin is shown (*, $p<0.01$). (F) The area of lung with fibrotic regions at each time point shown was calculated as the percentage of total lung area with fibrosis (*, $p<0.01$). (G) Representative IF analysis for CCSP (red), SPC (green), and DAPI (blue) in terminal bronchioles 21 days after bleomycin showing BASCs (arrowheads) in *Tsp1*$^{+/+}$ (left) and *Tsp1*$^{-/-}$ mice (right). (H) Quantification of BASCs as in C during bleomycin injury repair in *Tsp1*$^{+/+}$ (black bars) and *Tsp1*$^{-/-}$ mice (red bars). TBs, terminal bronchioles. Scale, 100um. Data presented are the mean of three individual mice. Error bars indicate standard deviation (*, $p<0.01$). Scale bar, 100um. See also Figure S6.